

Dual-frequency ultrasound-assisted alcohol/salt aqueous two-phase extraction and purification of *Astragalus* polysaccharides

Fadzai Chikari¹  | Juan Han¹ | Yun Wang² | Peng Luo¹ | Xingcheng He¹ | Emmanuel Kwaw³ | Phyllis Otu¹ 

¹School of Food & Biological Engineering, Jiangsu University, Zhenjiang, China

²School of Chemistry and Chemical Engineering, Jiangsu University, Zhenjiang, China

³School of Applied Sciences and Arts, Cape Coast Technical University, Cape Coast, Ghana

Correspondence

Juan Han, 301 Xuefu Road, Zhenjiang 212013, China.

Email: hanjuan@ujs.edu.cn

Funding information

National Natural Science Foundation of China., Grant/Award Numbers: 21676124, 21878131

Abstract

The study investigated the effect of dual-frequency ultrasound-assisted alcohol/salt aqueous two-phase extraction and desalination on the yield, microstructure and antioxidant properties of *Astragalus* polysaccharides (APS). Extracts were desalinated for 10 (APS₁₀), 20 (APS₂₀), and 30 (APS₃₀) minutes. A 28.40% experimental yield, well correlated to the response surface methodology predicted model was achieved. Thermodynamic parameters were non-spontaneous, irreversible and endothermic. Moreover, ultrasound enhanced the desalination rate and did not alter the chemical structure in the APS. Fourier Transform Infrared Spectroscopy showed a similar spectrum in all the APS samples. High-performance gel chromatography and scanning electron microscopy, respectively presented reduced molecular weights and altered microstructures in the samples. Monosaccharide analysis revealed the existence of xylose, mannose, galactose, glucose, arabinose, rhamnose, and ribose in the APS samples. Moreover, the APS₂₀ showed strong hydroxyl and 2,2-diphenyl-1-picrylhydrazyl radical scavenging activities, thus showing its potency in reducing oxidative stress. Hence, this study demonstrates that coupled ultrasound and alcohol/salt ATPS is a sustainable technique, which generates high yields of simultaneously extracted products.

Practical applications

Astragalus root has been used as an effective complementary treatment to conventional medicine owing to its rich nutraceutical composition and its numerous health attributes. Commercialization of *Astragalus* supplements into functional foods and nutraceuticals requires continuous exploration of novel, low cost and reproducible methods that retain their bioactivity. In this work, a synergized and bio-compatible dual-frequency ultrasound-assisted alcohol/salt aqueous two-phase system was used to extract and purify *Astragalus* polysaccharides. Application of this technique in the nutraceutical industry reduces treatment time, lowers bulk energy consumption hence reducing energy costs. It promotes the use of low-cost, non-hazardous bio-based solvents in treatment processes thus considerably reducing extraction costs and environmental degradation. Findings from this study exhibit the practicality of this technique in industrial application. It equips biotechnologists with

information on improved, sustainable and safer ways of extracting and enriching the quality of nutraceutical compounds.

1 | INTRODUCTION

Astragalus (*Huang qi*) belongs to the family of *Fabaceae* and its origin is traced to East Asia and Siberia. The root of the plant is of high value in Chinese Herbology due to its several potential health benefits in treating spleen related ailments; anorexia, fatigue, diabetes, common cold, diarrhea, cancer, cardiovascular and inflammatory diseases among others (Fu et al., 2014). Its therapeutic benefits have been ascribed to its rich nutraceutical composition (Sun et al., 2017). Recently, *Astragalus* polysaccharides (APS) have received increased attention, as a result of their ability to stimulate antioxidant enzymatic activities that degrade and stabilize free radicals thus reducing cellular oxidative impairment (Jin, Zhao, Huang, & Shang, 2014; Nimse & Pal, 2015). Besides, they exhibit anti-aging, anti-tumor and anti-hyperglycemic properties (Agyemang et al., 2013; Zhao et al., 2017). Over the past decades, various techniques have been employed to extract crude APS before purification. Zhu et al. (2011), reported a 9.77% yield using hot water extraction (HWE). However, high temperatures (>80°C) and longer extraction times (>1.5 hr) which effect structural degradation have narrowed its use (Wang, Zhang et al., 2019). To date, novel techniques such as microwave, ultrasound, and enzyme assisted extraction have been acknowledged to improve yields (>17%), reduce treatment time (<1 hr) and have lower energy costs (Bi & Wu, 2010). Nonetheless, the application of these robust techniques rouses the need to employ greater caution to preserve their biological structure pending purification. Therefore, there is a need to explore extraction techniques that retain the biological structure of extracted polysaccharides.

Purification of biomolecules remains a fundamental aspect of enriching the quality of extracted products. In the past decades, polymer/salt and polymer/polymer aqueous two-phase systems (ATPS) have been utilized in the purification of biomolecules (Liu, Zhu, & Fan, 2008). However, industrial upscaling of these systems remains compromised due to the exorbitant cost of polymers and the complexities of separating extracted molecules through back extraction processes (Goja, Yang, Cui, & Li, 2013). This has attracted a proliferation of studies around the alcohol/salt ATPS which have fast become key extracting systems in polysaccharide extraction and purification, due to their low viscosity, simple recovery mechanism, and cost-effectiveness (Iqbal et al., 2016). High recovery yields (<95%) and purification fold using alcohol/salt ATPS has been extensively reported (Ooi et al., 2009). Lately, the integration of ATPS with power ultrasound into a one-step extraction technique (UAATPS) has been acknowledged to improve polysaccharides yield. The synergistic effect of UAATPS through ultrasonic cell wall disintegration and diffusion of the solvent into the cell has a positive impact on the polysaccharide extract thus,

significantly increasing mass transfers of the active nutrients (Chemat & Khan, 2011; Ji, Peng, Yuan, Liu, & Wang, 2018). However, this technique has been associated with initiating the degradation of polysaccharides due to prolonged ultrasonic treatment (Dong et al., 2015). In recent times, alternative modes to mono frequency irradiation such as dual-frequency (DFu) have emerged and reported to have a better cavitation and product yield through a simultaneous effect of low and high frequencies (Muatasim, Ma, & Yang, 2018).

Although there are some reports on the effect of various extraction methods on the biological structure and functionality of *Astragalus* polysaccharides. There is a paucity of information on simultaneous extraction and purification of polysaccharides using the aqueous two-phase system under dual-frequency ultrasound (DFu-AATPS). Furthermore, no study has explored the thermodynamics of the APS using this technique. Thus, this study sought to investigate (a) the effects of simultaneous extraction and purification on the extraction yields, (b) the effects of dual-frequency ultrasound-assisted desalination on the microstructure and antioxidant properties of *Astragalus* polysaccharides, and (c) thermodynamic modeling of APS under dual-frequency ultrasound-assisted extraction.

2 | MATERIALS AND METHODS

2.1 | Materials and chemicals

Astragalus roots were obtained from Dingxi, Gansu Province China. Monosaccharide standards (D-glucose, D-galactose, D-mannose, D-xylose, L-arabinose, and L-rhamnose), Dextran T-series standards (T-10, T-40, T-70, T-500, T-1000, and T-2000), 2,2-diphenyl-1-picrylhydrazyl, Coomassie brilliant blue G-250, Bovine Serum Albumin (BSA), pyridine, hydroxylamine hydrochloride, acetic acid anhydride, trifluoroacetic acid, hydrogen peroxide, salicylic acid were purchased from Sigma-Aldrich Chemical Company (St Louis, MO). $(\text{NH}_4)_2\text{SO}_4$ and all other chemicals of analytical grade were purchased from Sinopharm Chemical Reagent Company (Shanghai, China). Distilled water was used in all experiments.

2.2 | Plant material preparation

Fresh *Astragalus* roots were obtained from Dingxi, Gansu Province China. Roots were washed to remove debris after which they were diced into 1-in. cubes and freeze-dried (-60°C, 48 hr, 0.02 mbar, FD-1A-50, Boyikang Laboratory Instruments, Beijing, China). Thereafter, the dried roots were powdered using a jet mill Model 0101S (Jet-O-Mizer Milling, Fluid Energy Processing and Equipment Company,

Telford) and sieved through a 20 mesh sieve (Chen, Zhou, & Zhang, 2014). The freeze-dried sample was stored in airtight polyethylene bags at 4°C prior to analysis.

2.3 | Pre-treatment of *Astragalus* root powder

Dried *Astragalus* powder was pretreated with 95% (v/v) ethanol in a Soxhlet apparatus (70°C, 5 hr) to remove pigments and lipophilic molecules. Subsequently, the treated powders were filtered, oven-dried at 40°C, and stored in an airtight polythene bag at room temperature for the following experiments.

2.4 | Simultaneous extraction and purification

Dual-frequency ultrasound-assisted aqueous two-phase extraction was performed in an ultrasonic reaction chamber with internal dimensions: 240 mm width × 207 mm length × 215 mm height, (Shangjia Biotechnology Co., Wuxi, Jiangsu, China), with three alternating dual frequencies. An ATPS composed of 29% (w/w) ethanol,

17% (w/w) (NH₄)₂SO₄ and 54% (w/w) distilled water was prepared in a 10 ml test tube and kept in a water bath (25°C, 12 hr) to completely dissolve the salt to form two phases. Subsequently, 20 mg of APS powder was added to the solution, vortexed and ultra-sonicated using the designed optimum conditions (270 W, 100% duty cycle, 20 and 40 kHz, 36°C, 40 min) as shown in Figure 1. Thereafter, the mixture was centrifuged (Anke KA-1000, Jiangsu Jinyi Instrument Technology Co. Ltd. Changzhou, Jiangsu, China) at 2000 rpm for 10 min at 4°C and kept at 25°C. After 12 hr, the salt-rich bottom phase and ethanol-rich top phase were separated using a Pasteur pipette. The total polysaccharide content of the bottom phase was analyzed using the phenol sulfuric acid method (Dubois, Gilles, Hamilton, Rebers, & Smith, 1956). A control sample without sample powder was prepared as blank to avoid interferences. Volume phase ratio and yield were calculated using the following equations:

$$\text{Volume ratio} = V_t/V_b \quad (1)$$

where V_t is volume in the top phase whilst V_b is the volume in the bottom phase.

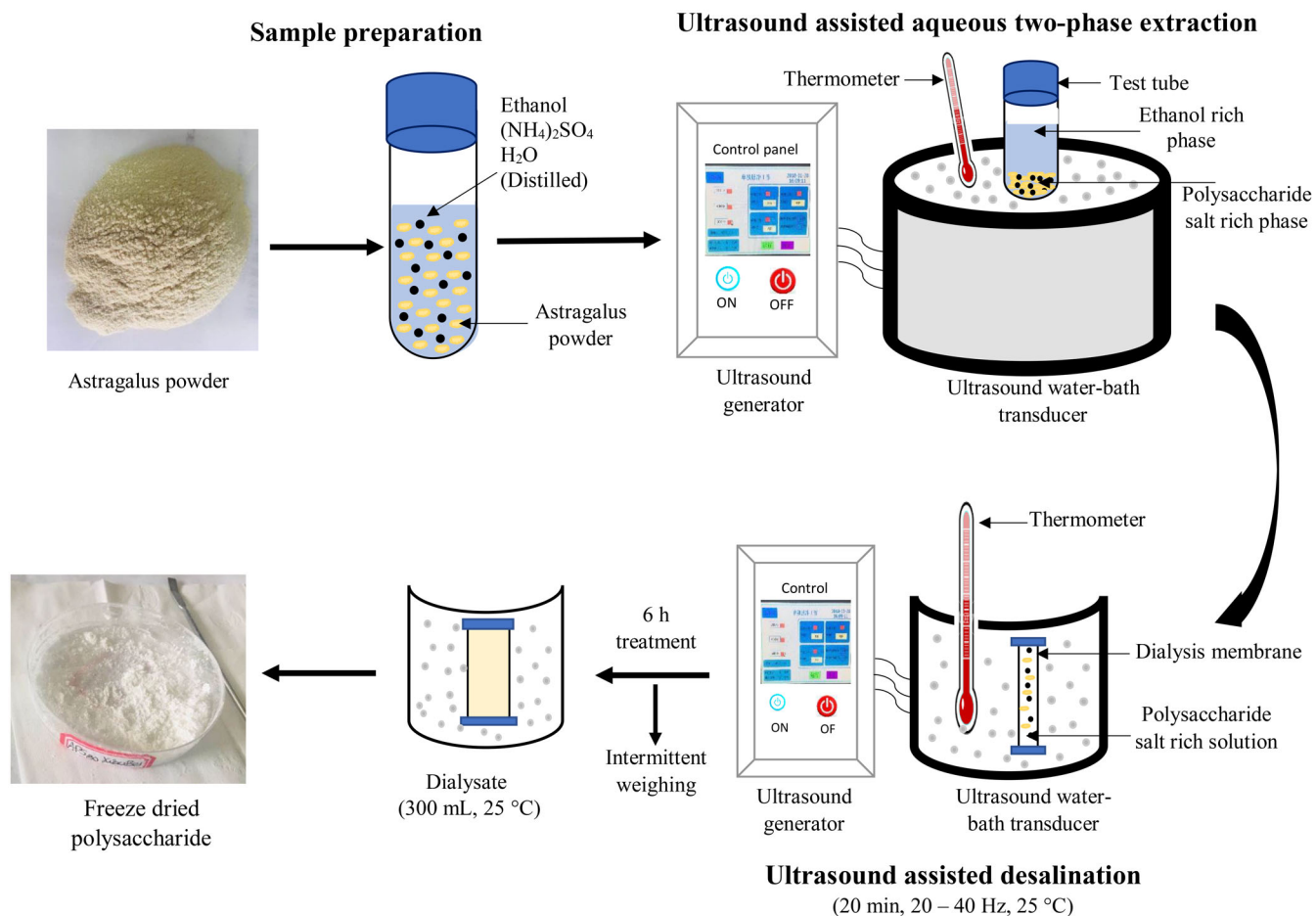


FIGURE 1 Schematic representation of extraction, purification, and desalination of *Astragalus* polysaccharides using combined dual-frequency ultrasound and ethanol/(NH₄)₂SO₄ ATPS

$$\text{Yield}(\%) = C \times V / W \times 100 \quad (2)$$

where C (mg/ml) represents the concentration of polysaccharides solution, while V (ml) is the volume of polysaccharide solution and W (g) is the mass of the sample after freeze-drying.

2.5 | Response surface methodology

A single factor design with extraction factors: X_1 -time (25–45 min), X_2 temperature (25–45°C), X_3 salt concentration (13–23%), X_4 ethanol concentration (21–31%), X_5 power (60–300 W), and X_6 frequency (20 and 40, 20 and 60, 40 and 60 kHz) was conducted and used as a guide in the selection of the key parameters for further

optimization experiments. Coded experimental factors X_1 (time), X_2 (temperature), X_3 (salt concentration), and X_4 (power) at three levels (−1, 0, +1) were fitted in a Box Behnken Design (BBD) to determine the optimal extraction conditions. All experiments were conducted in triplicate in a total of 29 runs as shown in Table 1. Results from the design were fitted to a quadratic polynomial model using the equation:

$$Y(\%) = \beta_0 + \sum_{i=1}^4 \beta_i X_i + \sum_{i=1}^4 \beta_{ii} X_i^2 + \sum_{j=i+1}^4 \beta_{ij} X_i X_j \quad (3)$$

where Y is the predicted response; β_0 , β_i , β_{ii} , and β_{ij} are the regression coefficients for the intercept, linearity, quadratic and the interaction of the model. X_i and X_j are independent variables.

Run	Independent variables (actual and coded)				Yield (%) Y
	Time (min) X_1	Temp. (°C) X_2	Salt conc. (%) X_3	Power (W) X_4	
1	40(1)	30(−1)	17(0)	240(0)	24.40
2	30(−1)	35(0)	19(1)	240(0)	23.24
3	30(−1)	30(−1)	17(0)	240(0)	24.50
4	35(0)	40(1)	17(0)	300(1)	24.63
5	40(1)	35(0)	17(0)	300(1)	27.82
6	35(0)	40(1)	15(−1)	240(0)	23.37
7	35(0)	35(0)	17(0)	240(0)	29.60
8	35(0)	35(0)	19(1)	300(1)	27.51
9	35(0)	30(−1)	19(1)	240(0)	23.35
10	35(0)	30(−1)	17(0)	180(−1)	20.27
11	35(0)	30(−1)	17(0)	300(1)	26.15
12	30(−1)	35(0)	17(0)	300(1)	24.99
13	35(0)	35(0)	15(−1)	300(1)	24.18
14	35(0)	40(1)	17(0)	180(−1)	19.53
15	40(1)	35(0)	17(0)	180(−1)	22.08
16	35(0)	35(0)	17(0)	240(0)	29.62
17	35(0)	35(0)	15(−1)	180(−1)	23.22
18	30(−1)	35(0)	15(−1)	240(0)	22.97
19	35(0)	35(0)	17(0)	240(0)	29.68
20	35(0)	30(−1)	15(−1)	240(0)	24.46
21	30(−1)	35(0)	17(0)	180(−1)	19.71
22	35(0)	40(1)	19(1)	240(0)	22.25
23	35(0)	35(0)	17(0)	240(0)	29.74
24	40(1)	35(0)	19(1)	240(0)	24.38
25	35(0)	35(0)	17(0)	240(0)	29.60
26	40(1)	40(1)	17(0)	240(0)	25.90
27	35(0)	35(0)	19(1)	180(−1)	17.78
28	30(−1)	40(1)	17(0)	240(0)	20.78
29	40(1)	35(0)	15(−1)	240(0)	27.20

TABLE 1 Box Behnken experimental design

2.6 | Desalination

Dual-frequency ultrasound-assisted desalination (DFu-AD) of the extracted and purified polysaccharides was conducted with minor modification using a method described by Otu, Haonan, Cunshan, and Hongpeng (2018). In brief, extracted samples of the polysaccharide salt-rich bottom phase were added to a dialysis membrane (8000–14,000 Da) and, coded as APS₁₀, APS₂₀, APS₃₀, and APS_{control}. Thereafter, samples were sonicated (20–40 kHz, 25°C 270 W) for 10, 20, and 30 min, respectively. Afterward, the dialysis membranes were put in a dialysate (300 ml distilled water) at 25°C and replaced every 30 min for the rest of the experimental time (350, 340, and 330 min, respectively). The change in weight (g) of the coded dialysis membranes was recorded every 30 min. A non-sonicated salt-rich bottom phase solution in the dialysis membrane coded as (APS_{control}) was kept in a water bath (30 min, 25°C), and further dialyzed for 330 min under normal room temperature with intermittent weighing and the dialysate being replaced after every 30 min. Initial and Change in weight of the dialyzed polysaccharide salt-rich bottom phase throughout the experimental time were used to construct a linear plot against time ($t/X_t - X_o$). The non-exponential Peleg's equation was used to calculate the equilibrium water content.

$$X_e = X_o + 1/K_2 \quad (4)$$

where X_e (g/g) is the equilibrium water content, X_o (g/g) is initial moisture content and K_2 is the constant from the intercept of a linear graph.

2.7 | Thermodynamics

Thermodynamic modeling of the APS extraction was explored for its feasibility to push the reaction in a forward direction. In this set of experiments two separate ATPS (29% (w/w) ethanol, 17% (w/w) (NH₄)₂SO₄ and 54% (w/w) distilled water) coded as APS and control were prepared. Subsequently, 20 mg of APS powder was added and vortex mixed. Using optimized conditions the coded APS sample was ultra-sonicated (20 and 40 kHz, 270 W, and 25°C) at varying temperatures (10–30°C). Conversely, the control sample was extracted in a water bath (30°C) at varying temperatures. Experimental results were used to plot a linear graph of $\ln(K)$ against $1/T$ (K) and $\ln(F)$ against $1/T$ (K). According to the Arrhenius equation (Liau et al., 2008). The activation energy (E_a) was calculated using the following equation:

$$k = Ae^{-E_a/RT} \quad (5)$$

where k is rate constant, E_a (KJ/mol) is the activation energy, R is gas constant, T is extraction temperature, and A is Arrhenius constant.

The reaction characteristics of enthalpy (ΔH), entropy (ΔS), and Gibbs activation energy (ΔG) in the APS extraction were calculated using Equation (6) (Liau et al., 2008) and Equation (7) (Salehi, Kashaninejad, Tadayyon, & Arabameri, 2015)

$$\ln F = -\frac{\Delta G}{R} \frac{1}{T} = -\frac{\Delta H}{R} \frac{1}{T} + \frac{\Delta S}{R} \quad (6)$$

$$F = \frac{Y_T}{Y_U} \quad (7)$$

where F is equilibrium constant, Y_T is the polysaccharide yield percent at temperature T , Y_U is the un-extracted percentages of APS, R , is a gas constant (8.3145), ΔH , (kJ/mol) is enthalpy, ΔS , (kJ/mol K) is entropy, and ΔG , (kJ/mol) is a free energy of extraction. ΔG was estimated using the slope of $\ln(F)$ while ΔS was calculated using the intercept.

2.8 | Chemical analysis

Total polysaccharide and protein content in the APS samples were estimated using the Phenol Sulfuric (Dubois et al., 1956), the Bradford method (Bradford, 1976). D-glucose and Bovine serum albumin were used as standards for the polysaccharide and protein content, respectively. Absorbance was read at 490 nm for the polysaccharide and 595 nm for the protein using a UV spectrophotometer (UV-1600, Beijing Rayleigh Analytical Instrument, Beijing, China).

2.9 | Physicochemical analysis

2.9.1 | Monosaccharide composition

The monosaccharide composition of the APS was determined by Gas Chromatography (GC). The sample was prepared using a method previously described by (Chen et al., 2015). In brief, 10 mg of the APS was hydrolyzed with 2 M of trifluoroacetic acid (TFA) at 121°C for 5 hr. Subsequently, the solution was concentrated in a vacuum and methanol was used to remove the excess acids before acetylation. Afterward, 10 mg of hydroxylamine hydrochloride and 0.5 ml pyridine were heated (90°C, 25 min), then cooled at normal room temperature. Consequently, 0.5 ml of acetic acid anhydride was added to the solution, vortexed, further kept in a water bath (90°C, 25 min) then allowed to cool at room temperature again. After cooling, 1 μ l of the supernatant was injected into a SE-54 capillary column (30 m \times 0.32 mm \times 0.5 μ m) and analyzed using an Agilent Technologies 7890 GC system (Agilent Technologies). The analysis was conducted under the operating conditions: N₂ carrier gas rate 1 ml/min; detection and injection temperature was 240°C; column temperature 170°C for 2 min then adjusted to 240°C at 6°C/min, then lastly held at 240°C for 10 min.

2.9.2 | Molecular weight

Molecular weight (MW) of the APS was determined by gel permeation chromatography (GPC) according to a method previously described by

(Pu et al., 2016) with slight modification. The instrument was equipped with an LC20 high-performance liquid chromatography pump with a RID-20 difference refractive index detector (Japan Shimadzu Company). HR4 Styragel columns (Waters Corp, Milford, MA) were used at an oven temperature of 35°C. In brief, 30 µL of the APS sample was injected and eluted with a mobile phase constituted of 0.05 M NaNO₃ and 0.01% NaN₃ solution under the following operating conditions: flow rate of 0.7 ml/min, column temperature of 35°C and running time of 20 min. The calibration curve and molecular weight of the polysaccharides were calculated using Dextran T-series standards (T-10, T-40, T-70, T-500, T-1000, and T-2000).

2.9.3 | Morphological structure of polysaccharides

The purified samples were coated with gold-palladium and scanned under a scanning electron microscope (JSM-6010 PLUS/LA, Japan).

2.10 | Spectral analysis

2.10.1 | FTIR analysis

The infrared spectrum of the APS₁₀, APS₂₀, APS₃₀, and APS_{control} were determined using a Fourier Transform IR spectrophotometer (Nicolet Nexus 470). APS samples were mixed with pre-dried potassium bromide (110°C, 6 hr) (1:100 mg). Thereafter, the mixture was ground and pressed into thin pellets and scanned in a range 4,000–400 cm⁻¹.

2.10.2 | UV-vis analysis

Ultraviolet scanning was conducted using a UV-Vis spectrophotometer (Cary 8,454 Agilent Company). Concisely, the APS samples were dissolved in distilled water (2 mg/ml) and absorbance was recorded between 200–400 nm. Distilled water was used as a blank.

2.11 | Radical scavenging activity assays

2.11.1 | Hydroxyl radical scavenging activity

Hydroxyl scavenging activity of APS was conducted with minor modifications to a method described by (Pu et al., 2016). In brief, different concentrations (0.2–1.4 mg/ml) of the APS sample were prepared. 0.5 ml of each concentration was added to a working solution of 0.5 ml salicylic-ethanol solution (10 mmol/L), 0.5 ml Iron II sulfate (9 mmol/L), and 1 ml of H₂O₂ in different test tubes. Consequently, the mixture was incubated for 30 min at 25°C and absorbance was read at 510 nm. Scavenging activity was estimated using the following equation:

$$\text{Scavenging activity (\%)} = \frac{A_0 - (A_1 - A_2)}{A_0} \times 100 \quad (8)$$

where A₀ is the absorbance of the control sample, A₁ is absorbance of the APS sample, and A₂ is the absorbance of the sample without the salicylic-ethanol solution.

2.11.2 | DPPH radical scavenging activity

The 2,2-diphenyl-1-picrylhydrazyl radical scavenging activity (DPPH-SA) of the APS was determined as described by (Osae et al., 2019) with slight modifications. In essence, 0.5 ml APS solution at varied concentrations (0.2–1.4 mg/ml) were prepared and added to 1 ml of DPPH-ethanol solution (0.08 mg/ml) and vortexed for 1 min. Consequently, the solution was kept in the dark for 30 min at 25°C after which the absorbance was read at 517 nm. A blank solution with ethanol and DPPH was used as control. Inhibition was estimated using the equation:

$$\% \text{DPPH} = \left(\frac{A_0 - A_1}{A_0} \right) \times 100 \quad (9)$$

where A₀ is the absorbance of the control and A₁ is the absorbance of the APS sample solution.

2.12 | Statistical analysis

All experiments and assays were performed in triplicate for accuracy and results were presented as mean ± SD. One-way Analysis of variance (ANOVA) was performed using OriginPro version 2015 (OriginLab, Northampton). Tukey test was used to compute statistically significant differences at *p* < .05.

3 | RESULTS AND DISCUSSION

3.1 | Single-factor experiments

3.1.1 | Effect of temperature on APS yield

The extraction temperature was a contributing factor to the solubility of the polysaccharides and viscosity of the two-phase system. As displayed in Figure 2a, extraction conditions (DFu (20–60 kHz), time (30 min), power (300 W), 29% ethanol and 19% (NH₄)₂SO₄ concentration) were kept constant to determine optimum extraction temperature. It was observed that an increase in temperature from 20–35°C resulted in an increase in the APS yield while temperature greater than 35°C reduced the APS yield. The increases in yield can be ascribed to the increased sonochemical effects that occur at low temperatures which increases the diffusion of the polysaccharides into the solvent. Lower temperatures simplify the cavitation process by

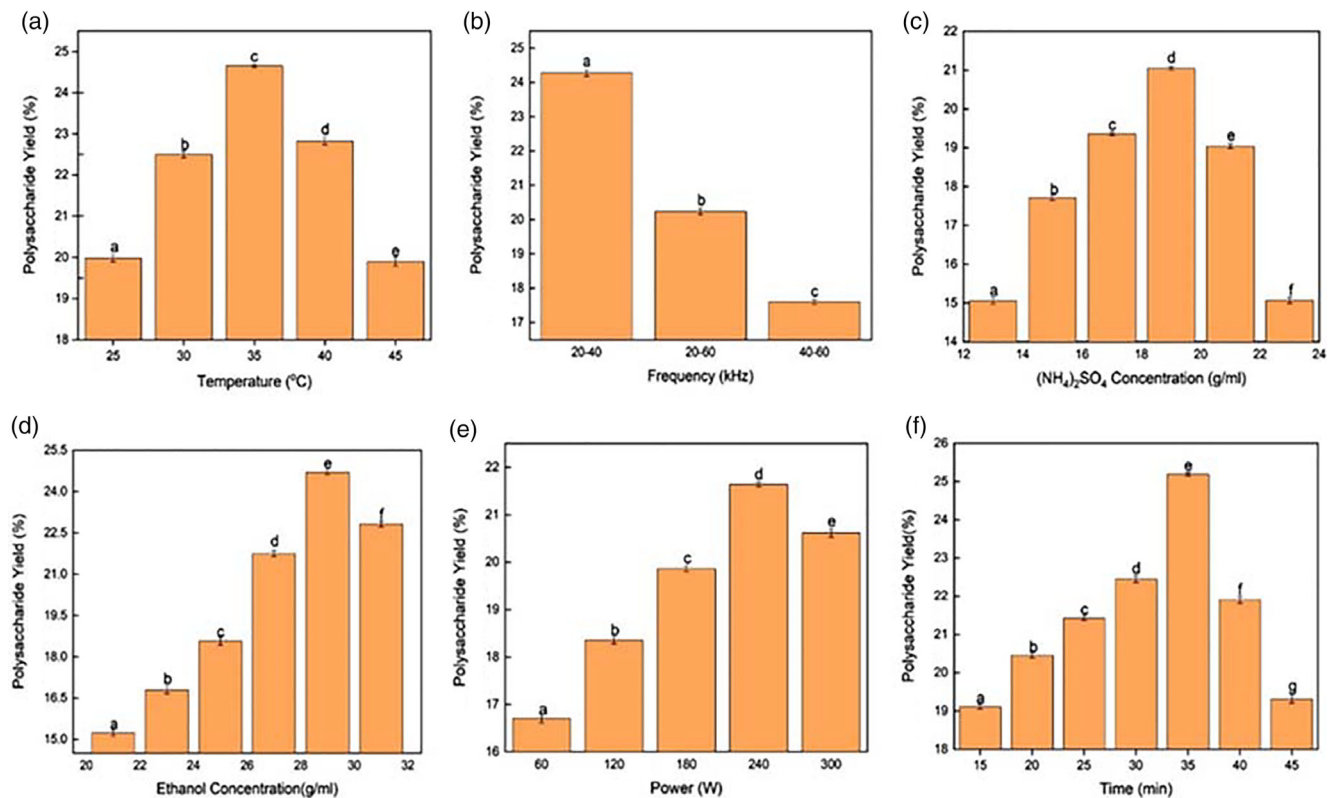


FIGURE 2 Effect of extraction temperature; ultrasound frequency; salt concentration; ethanol concentration; ultrasound power and extraction time on the yield of *Astragalus* polysaccharides

increasing the surface tension and viscosity of the solvent, thus improving the solvent/material interaction and attaining maximum cavitation efficiencies (Wang, Fan, Wang, Zhang, & Wang, 2018). On the other hand, as the temperature rises surface tension, and viscosity of the solvent gradually decrease, this then slows down the solubility and transfer of the active polysaccharides (Yan, Wang, Qiu, Wang, & Ma, 2018). Moreover, increment in temperature induces the solvent vapor pressure to rise and fill up the cavitation bubbles thus weakening the cavitation process and reducing the rate of bubble formation and collapse. This phenomenon accounts for a longer extraction process which potentially induces degradation of the polysaccharides (Capelo-Martínez, 2009; Zhang et al., 2008).

3.1.2 | Effect of dual-frequency ultrasound on APS yield

The optimum frequency was investigated and the result is shown in Figure 2b. The results revealed that the frequency of 20 and 40 kHz led to maximum yield. The findings could be attributed to the concurrent waves of ultrasonic irradiation which have been reported to have a positive outcome on acoustic cavitation (Kalinenko, Baklanov, & Makarov, 2016). Furthermore, the phenomena of low frequencies enable maximum cavitation which induces vigorous cell disintegration, thereby increasing the diffusion of targeted products into the solvent (Chemat & Khan, 2011). According to Feng, Zhao, Zhu, and Mason

(2002), a frequency difference of 20 kHz in the acoustic field intensifies the generation of higher amplitude which is best suited for ultrasonic irradiation. The aforementioned could explain the reason for the high yield at a dual-frequency of 20–40 kHz. The result is supported by that of Muatasim et al. (2018), who reported that enhanced cavitation efficiencies in dual-frequency (20–40 kHz) resulted in a significant yield of 38.93% crude polysaccharides from *Lycium barbarum*.

3.1.3 | Effect of salt concentration on APS yield

Optimal salt concentration was studied with varying (NH₄)₂SO₄ (13–23% w/w) while other extraction factors were kept constant (ethanol (29%), temperature (30°C) dual-frequency (20 and 60 kHz) and power (300 W). As shown in Figure 2c, an increment in the salt concentration 15–19% resulted significant ($p < .05$) increase on the APS yield. In our case increasing the salt concentration led to a heterogeneous solution, it increased the volume of the top phase and influenced the partitioning of the APS in the ethanol-top phase. This finding can be ascribed to the salting-out principle (Guo, Han, Zhang, Wang, & Zhou, 2013). Previous studies have reported that increasing salt concentration in an alcohol/salt APTS eliminates the lower molecular weight molecules from the bottom phase into the alcohol rich phase (Wang, Han, Xu, Hu, & Yan, 2010). However, further addition of (NH₄)₂SO₄ beyond 19% had a detrimental effect on the APS yield. This might have been caused by the saturation of (NH₄)₂SO₄ in the

top phase. We related this result to the ion-dipole phenomena (Guo et al., 2013), which caused the APS to partition to the salt-rich bottom phase. The hydration of the salt ions consequently caused the $(\text{NH}_4)_2\text{SO}_4$ to be dissolved in the bottom phase thus decreasing the volume of water in the bottom phase. Guo et al. (2013), reported a similar observation in the extraction of lignans from *Schisandra chinensis*.

3.1.4 | Effect of ethanol addition on APS yield

The effect of ethanol addition was studied in a range (21–31%). As illustrated in Figure 2d, a significant rise in yield was observed when ethanol concentration increased. The maximum yield was obtained at 29% (w/w) when all other conditions were fixed. An increase in ethanol concentration intensifies the solubility and partitioning of ethanol-soluble polysaccharide to the top phase consequently, increasing the extraction efficiency (Guo et al., 2013). However, further increment in ethanol concentration above 29% induced salt precipitation and caused a decrease in the APS yield, thus 29% (w/w) was selected for the optimization experiments.

3.1.5 | Effect of ultrasound power on APS yield

The previously determined extraction conditions, time (30 min), temperature (30°C), dual-frequency (20–40 kHz), ethanol concentration (29%), and $(\text{NH}_4)_2\text{SO}_4$ (19%) were kept constant while ultrasonic power was varied (60–300 W). The results in Figure 2e showed a maximum APS yield at 240 W with a decrease in yield beyond 240 W. The decrease in the APS yield when power exceeded 240 W could be ascribed to the exaggeration of the amplitude of the ultrasound wave thus inducing a vigorous generation of cavitation bubbles which reduces the transmission of ultrasonic energy into the cavitation field leading to a decrease in the APS yield (Ponmurugan et al., 2017). Therefore the optimal power of 240 W was chosen for subsequent experiments.

3.1.6 | Effect of extraction time on APS yield

Keeping previously determined factors constant, the effect of extraction time on the yield of APS was studied. Our findings showed that an increase in time led to an increase in APS yield as shown in Figure 2f. Possible reasons for the increase in yield could be related to improved solubilization and diffusion of polysaccharides into the extracting solvent with time, while the mechanical effects of ultrasound technology could have increased cavitation efficiencies thereby increasing the surface area for solubility of the purified APS (Zhao, Yang, Liu, Zhao, & Wang, 2018). However, a decline in yield was observed beyond 35 min and this could be ascribed to the effect of ultrasonication on the glycosidic bonds. Throughout the sonication process, the chemical structure of the polysaccharides remains unaltered while the glycosidic bonds are destroyed consequently

reducing the molecular weight and polymer chains (Ogotu, Mu, Elahi, Zhang, & Sun, 2015; Zhang et al., 2013). Ji et al. (2018) reported a significant reduction in *Ziziphus jujuba* polysaccharide yield beyond 38 min which they attributed to polysaccharide hydrolysis due to a higher temperature and extended sonication time.

3.2 | Optimization

3.2.1 | Model fitting

Adequately selected models were evaluated by fitting Box Behnken experimental results into linear and quadratic models using Analysis of Variance (ANOVA). As summarized in Table 2, a significant ($p < .0001$) second-order polynomial model was illustrated. Linear factors (X_1, X_2, X_3, X_4), quadratic factors X_1^2, X_2^2, X_3^2 and interactive factors X_1, X_2, X_1X_3 , and X_3X_4 all exhibited significance. A coefficient of determination R^2 (.998) and adjusted R^2 (.995) which showed high statistical significance demonstrated a correlation between the experimental factors and polysaccharide yield. The lack of fit from the estimated p -value was non-significant (.2065) relative to a pure error in the fitness of the model which depicts a suitable model (Kwaw et al., 2017). The experimental data obtained from BBD was analyzed by multiple regression equation and fit the second-order polynomial model:

$$Y_1 = 29.64 + 1.30X_1 - 0.56X_2 - 0.57X_3 + 2.72X_4 + 1.31X_1X_2 - 0.77X_1X_3 + 0.12X_1X_4 - 0.0023X_2X_3 - 0.20X_2X_4 + 2.19X_3X_4 - 2.35X_1^2 - 3.40X_2^2 - 2.86X_3^2 - 3.61X_4^2 \quad (10)$$

3.2.2 | Response surface analysis

To illustrate the correlation of the independent variables influencing the APS yield, 3D surface plots were constructed. The integration of response surface and analysis of variance displayed in Tables 1 and 2 revealed a strong interaction between $X_1X_2, X_1X_3, X_1X_4, X_2X_4$, and X_3X_4 as presented in Figure 3.

As shown in Figure 3a, a mutual interaction effect of X_1X_2 had a positive significant ($p < .001$) effect on the APS yield. An increase in X_1 and X_2 led to the peak cavitation threshold and intensified the APS yield. Lower temperatures provide a conducive environment for sonochemical effects to occur, thus maximum cavitation and improved extraction efficiency was achieved (Capelo-Martínez, 2009). Extended ultrasonic treatment conditions (higher temperature and time) might have led to polysaccharide loss and a reduction in the APS yield. These results are in agreement with previous studies of Zou, Jiang, and Tian (2015), who reported that long ultrasonic time and high temperatures led to a reduction in yield.

Figure 3b displays a significant ($p < .001$) effect of interactive factors X_1X_3 on the APS yield. This result demonstrated that maximum solubility and transfer of polysaccharides was achieved with a rise in time towards (35 min) and $(\text{NH}_4)_2\text{SO}_4$ concentration (17%). Reduction in yield at higher levels towards (40 min and 19%) compromised the

TABLE 2 Analysis of variance (ANOVA) for the experimental results of the Box-Behnken

Source	Sum of squares	df	Mean square	F value	p-Value
Model	307.87	14	21.99	4,004.82	<.0001***
<i>Linear</i>					
X_1	20.22	1	20.22	3,682.25	<.0001***
X_2	3.7	1	3.7	674.71	<.0001***
X_3	3.93	1	3.93	715.92	<.0001***
X_4	89.01	1	89.01	16,210.28	<.0001***
<i>Interactions</i>					
X_1X_2	6.82	1	6.82	1,241.45	<.0001***
X_1X_3	2.38	1	2.38	433.54	<.0001***
X_1X_4	0.054	1	0.054	9.75	.0075*
X_2X_3	2.07×10^{-05}	1	2.07×10^{-05}	3.77×10^{-03}	.9519
X_2X_4	0.16	1	0.16	28.56	.0001**
X_3X_4	19.23	1	19.23	3,501.78	<.0001***
<i>Quadratic</i>					
X_1^2	35.91	1	35.91	6,540.34	<.0001***
X_2^2	75.01	1	75.01	13,660.85	<.0001***
X_3^2	53.04	1	53.04	9,658.86	<.0001***
X_4^2	84.73	1	84.73	15,429.92	<.0001***
Lack of fit	0.066	10	6.59×10^{-03}	2.4	.2065
R^2					.9998
Adj. R^2					.9995
Pred. R^2					.9987
% CV					.30
AP					224.455

Note: X_1 —time (min); X_2 —temperature ($^{\circ}$ C); X_3 —salt concentration (%w/w); X_4 —power (W).

Abbreviations: AP, adequate precision; CV, coefficient of variation; Y, yield (%).

*Significant at $p < .05$.; **Significant at $p < .001$.; ***Significant at $p < .0001$.

solubility of $(\text{NH}_4)_2\text{SO}_4$ and distribution of polysaccharides in the top phase due to saturation, while prolonged ultrasonic exposure consequently led to structural loss (Guo, Han, Zhang, Wang, & Zhou, 2012).

As displayed in Figure 3c, a positive interactive effect of X_1X_4 could have contributed to a significant rise in the APS yield as a result of improved solubility and mass transfers of polysaccharides with an increase in sonication time and power. However, a decline in yield beyond 35 min and 240 W might have led to structural changes due to extended treatment time and extremely high amplitudes (Capelo-Martínez, 2009).

The significant ($p < .001$) synergistic interaction of X_2X_4 displayed in Figure 3d shows that optimum extraction yield was attained with an increase in temperature to (35° C) and power (240 W). This outcome can be related to the enhanced interaction of macromolecules with extracting solvent due to increasing ultrasonic power (Wang, Zhang et al., 2010). The reduction in yield beyond 240 W and 35° C led to polysaccharide degradation as a result of higher ultrasonic power and temperature.

The 3D plot of X_3X_4 shows a negative effect on the yield. As illustrated in Figure 3e, an increase in power at a high salt concentration (17%) led to an increase in the APS extraction yield. The relatively high power could have influenced the solubility and increased the partitioning of polysaccharides to the top phase of the ATPS. However, a decrease in APS yield occurred at a high salt concentration above 17% with a power of

300 W. This could be attributed to the poor partitioning of polysaccharides to the bottom phase due to the salting effect (Wang, Zhang et al., 2010).

3.2.3 | Validation of the model

The optimal extraction parameters were established to obtain the maximum yield. Based on these predicted conditions: time, $X_1 = 40$ min, temperature, $X_2 = 35.5^{\circ}$ C, $(\text{NH}_4)_2\text{SO}_4$, $X_3 = 16.81\%$ (w/w) and power, $X_4 = 262$ W a corresponding yield of 29.19% was to be obtained. Using modified conditions: $X_1 = 40$ min, temperature, $X_2 = 36^{\circ}$ C, $X_3 = 17\%$ $(\text{NH}_4)_2\text{SO}_4$ (w/w) and power, $X_4 = 270$ W, the experimental result obtained was $28.40 \pm 1.05\%$. The results are close to the predicted values of the model within a 95% confidence interval. Therefore, confirming the suitability, validity, and reproducibility of the models.

3.3 | Primary characterization of APS polysaccharides

The preliminary characterization of the freeze-dried samples is displayed in Table 3. From the results, it was observed that

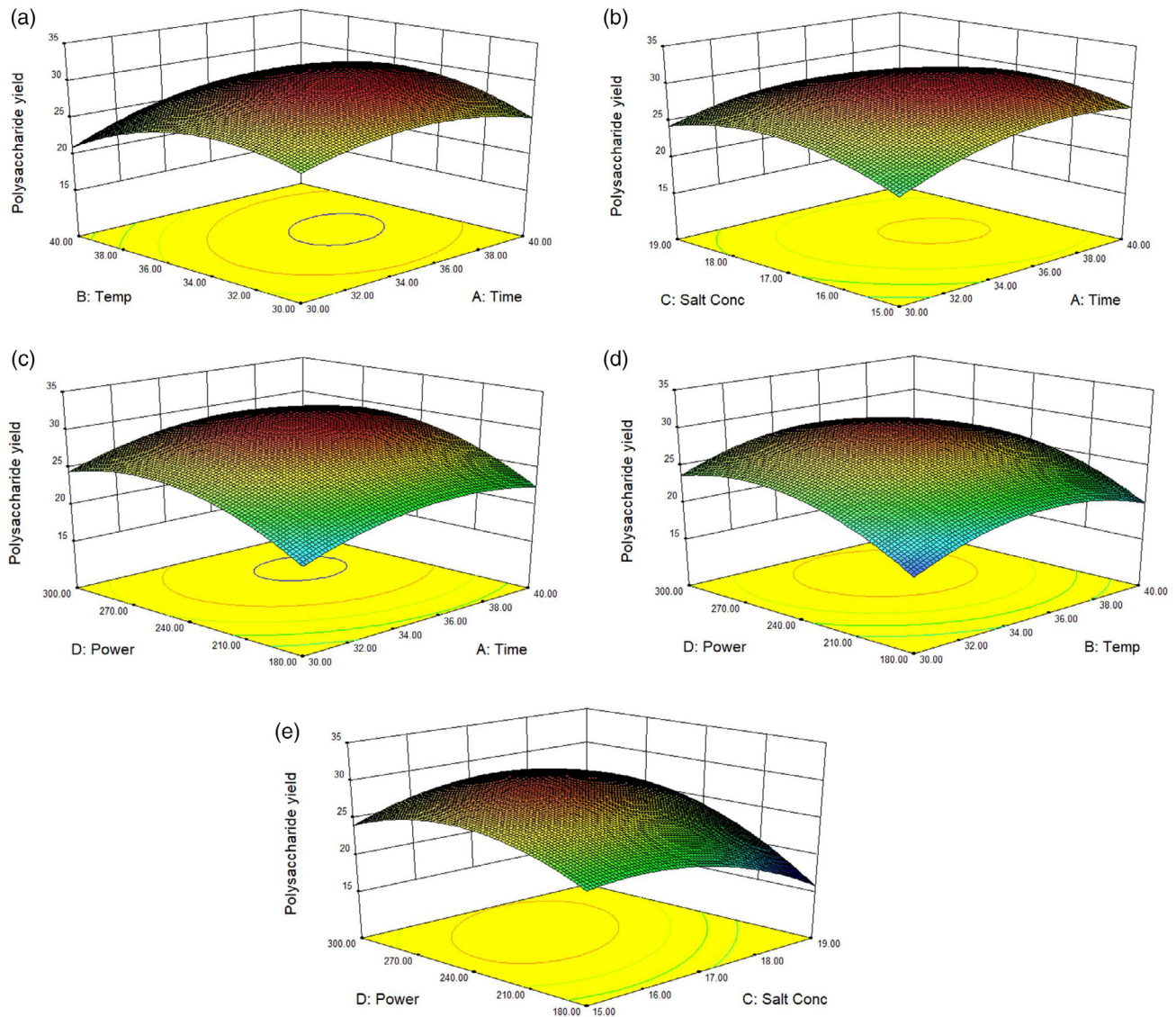


FIGURE 3 Response surface plots displaying the effect of extraction variables X_1 time (min), X_2 —temperature ($^{\circ}\text{C}$), X_3 —salt concentration (%), and X_4 —power (W) on the APS yield

ultrasonication did not have a major effect on the chemical composition of the APS samples. This is shown by the higher carbohydrate and lower protein content (%) of the DFu-AD samples (APS₁₀, APS₂₀, APS₃₀) comparing with the non-sonicated APS_{control} sample. The results can be ascribed to an effective deproteinization using the ethanol/ $(\text{NH}_4)_2\text{SO}_4$ ATPS (Wu, Li, Zhao, & Liu, 2017), and a robust desalination process, that was effective in removing a substantial amount of salt into the dialysate which was replaced after every 30 min throughout the experimental time.

3.4 | Thermodynamics

Dual-frequency sonication had a positive effect on energy transfer in the APS extraction. The use of ultrasound as additional energy in the extraction process considerably contributed towards attaining an endothermic,

TABLE 3 Physicochemical characterization of *Astragalus* polysaccharides

Sample	Carbohydrate (%)	Protein (%)
APS ₁₀	71.10	0.61
APS ₂₀	72.90	0.68
APS ₃₀	74.90	0.75
APS _{control}	66.96	2.66

Note: APS₁₀—ultrasound treatment (10 min), APS₂₀—ultrasound treatment (20 min), APS₃₀—ultrasound treatment (30 min), APS_{control}—ultrasound treatment (0 min).

non-spontaneous and irreversible reaction process. As displayed in Figure 4, high coefficients of determination (R^2) values were observed in the APS sample in both plots of $\ln(K)$ 0.9871 and $\ln(F)$ 0.9865, this can be related to the cavitation phenomena which enhanced the extraction

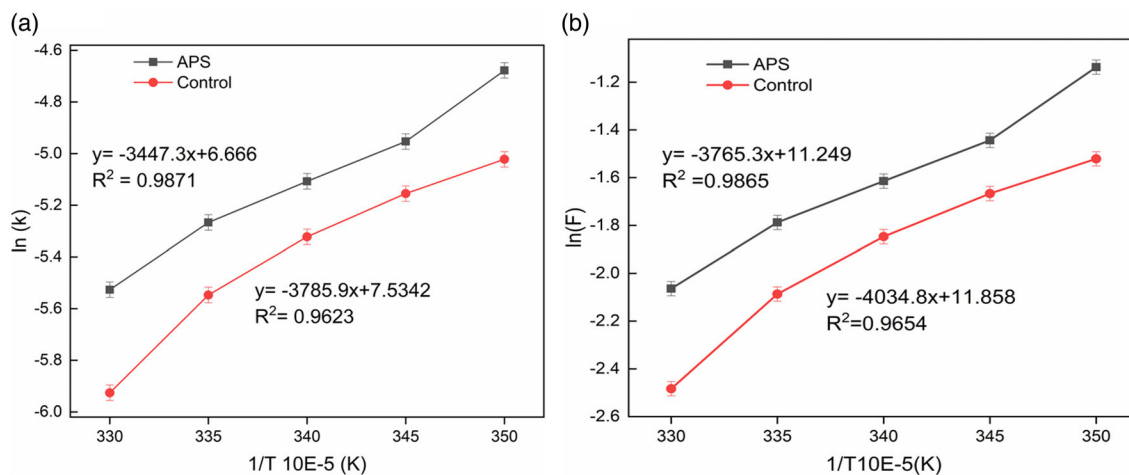


FIGURE 4 Thermodynamic graph of APS extraction: (a) energy of activation (E_a) (KJ/mol); (b) enthalpy of activation (ΔH) (KJ/mol), entropy of activation (ΔS) (KJ/mol K), Gibbs free energy (ΔG) (KJ/mol)

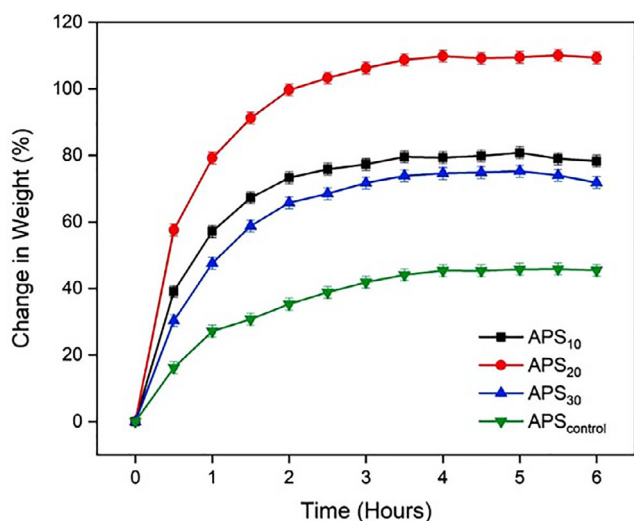


FIGURE 5 Dual-frequency ultrasound-assisted desalination of polysaccharide-salt rich bottom phase solution

efficiency. Activation energy values were reported as 28.66 and 31.47 kJ/mol for APS and the control, respectively. Entropy and enthalpy values for the APS were reported as 0.0935 and 31.06 kJ/mol, while Gibbs activation energy for the APS was also reported within the range of 4.84 kJ/mol to 2.97 kJ/mol. Our results are similar to those reported by Wang, Zhang et al. (2019) who indicated that ultrasonic treatment led to non-spontaneous, endothermic and irreversible reactions in the extraction of polysaccharides from *Glycyrrhiza*.

3.5 | Desalination

Dual-frequency ultrasonic irradiation significantly ($p < .05$) improved the desalination rate as shown in Figure 5. Ultra-sonicated samples displayed a high change in weight (%) from 71% for APS₃₀ to 78.3% and 109% for APS₁₀ and APS₂₀, respectively. However, the non-

sonicated control sample presented the lowest desalination rate of 45.45%. The increase in the desalination rate of sonicated samples could be attributed to the use of ultrasound transducers which facilitated the creation of a strong cavitation process that was able to inhibit clogging of the membrane, and take out concentration-polarization throughout water desalination (Feng, Van Deventer, & Aldrich, 2006). However, a decline in the change of weight in APS₃₀ could be due to extended sonication time (30 min) and a higher ultrasound intensity which potentially disturbed the permeability of the membrane and this might have led membrane rupture (Wang, Li, Fu, Chen, & Gao, 2005). The absence of sonication in the APS_{control} could have compromised the effective removal of salt from the salt-rich bottom phase. In a previous study, Zhou, Zhang, Fang, and Liu (2015) reported a 10% increase in desalination rate under DFu-UAD, thus confirming our results.

3.6 | Structural composition

3.6.1 | Monosaccharide composition

Monosaccharide composition of the APS was analyzed using Gas chromatography and the monosaccharides in the APS hydrolysates were confirmed by matching them with the retention times of the standards. Table 4 presents the relative contents and retention times of the identified monosaccharides in the APS samples. GC analysis revealed the dominance of xylose, arabinose, glucose, mannose in all the APS samples with higher relative contents of arabinose and glucose being observed in the APS_{control}, while xylose was the dominant monosaccharide in the APS₂₀. However, smaller amounts of ribose, rhamnose, and galactose existed in the APS₁₀ and APS_{control}. The dominance of xylose, arabinose, and glucose in the APS further confirms the APS as neutral polysaccharides as there were no uronic acids detected and observed. Findings from our investigation are in line with a number of research studies who have reported that *Astragalus*

TABLE 4 Relative content and retention time of the monosaccharide composition of the purified *Astragalus* polysaccharides

	D-ribose	L-rhamnose	L-arabinose	D-xylose	D-mannose	Glucose	Galactose
Sample retention time (min)	7.648	7.763	7.958	8.11	10.513	10.629	10.944
APS ₁₀ relative content	9.45	/	23.20	8.79	15.67	12.94	29.95
APS ₂₀ relative content	/	13.58	16.35	18.70	18.61	15.70	17.05
APS ₃₀ relative content	/	/	24.16	13.05	39.21	23.58	/
APS _{control} relative content	10.97	6.82	35.18	16.29	/	30.74	/

Note: APS₁₀—ultrasound treatment (10 min), APS₂₀—ultrasound treatment (20 min), APS₃₀—ultrasound treatment (30 min), APS_{control}—ultrasound treatment (0 min).

Sample	Elution time (min)	M _w (kDa) ^a	M _n (kDa) ^a	M _z (kDa) ^a	M _w /M _n ^a
APS ₁₀	15.559	11.433	8.1182	16.1597	1.408
APS ₂₀	15.546	11.454	8.1204	16.1620	1.410
APS ₃₀	18.277	10.203	7.1605	14.0931	1.424
APS _{control}	15.031	12.650	9.3940	19.0937	1.346

TABLE 5 Molecular weight parameters of APS₁₀, APS₂₀, APS₃₀, and APS_{control}

Abbreviations M_n, number-average molecular weight; M_w, weight-average molecular weight; M_w/M_n, molecular weight distribution; M_z, Viscosity-average molecular weight.
^amolecular weight parameters.

polysaccharides are commonly constituted of monosaccharides such as glucose, arabinose, galactose, mannose, rhamnose, xylose, fucose, fructose, and ribose while galacturonic and glucuronic acid might also be existent (Jin et al., 2014; Wang, Jia et al., 2019).

3.6.2 | Molecular weight determination (HPGPC)

The effects of dual-frequency ultrasound-assisted desalination (DFu-AD) on the molecular weight of the APS were studied and the results are presented in Table 5. From our findings, it was observed that DFu-AD considerably reduced the molecular weights (MW) of the APS samples. The phenomena of sonication using low frequencies and high-intensity ultrasound produce shear forces that contribute to the breaking of covalent bonds in the APS thus degrading polysaccharide molecules and reducing their molecular weight (Peres, Leite, & Silveira, 2015). However, extended ultrasonic treatment potentially damages the polysaccharide-molecular chain, induces degradation of molecules and as a result, affect the bioactivity of the extracted polysaccharides (Zhu et al., 2014). Our observation is consistent with that of Liu, Zhang, Xu, and Zhang (2013), who reported a drastically degraded molecular structure and reduced MW of pectin from apples after ultrasound treatment.

3.6.3 | Scanning electron microscopy

The microstructure of desalinated polysaccharides is illustrated in Figure 6. The effect of dual-frequency ultrasound in the desalination process was evidently displayed by the shape and structural changes. The non-sonicated APS_{control} sample displayed a corresponding

network like structure (Otu et al., 2018). Sonicated samples displayed a partial networking and fragmented structure in the APS₁₀, continuous irradiation resulted in a rod-shaped and an uneven aggregated structure in the APS₂₀, while a totally aggregated and damaged structure was observed in the APS₃₀ (Ying, Han, & Li, 2011). The significant differences in the structures can be attributed to the impact of acoustic cavitation and increased treatment time which jointly damaged the polysaccharides cell wall thus effecting structural changes. Wang, Wang, and Guo, (2019) alluded to significantly modified structures with ultrasound treatment as compared to non-ultrasound treatment.

3.7 | Spectral analysis

3.7.1 | Fourier transform-infrared spectroscopy

Spectral analysis of the APS samples was similar with minor differences in the intensity of the peaks. As displayed in Figure 7a, a strong absorption peak observed at 3237 cm⁻¹ was linked to hydroxyl stretching vibration of the polysaccharides in hydrogen bonds (Guo & Wu, 2008). A band at 2362 cm⁻¹ was typical of C-H stretching and bending vibration (Luo et al., 2010). Carboxylic acid compounds were characterized by a band at 1410 cm⁻¹ which was attributed to the C=O bending vibration. Bands within 1,000–1,200 cm⁻¹ were typical of C—O—H and C—O—C stretching vibrations (Kacurakova, Capek, Sasinkova, Wellner, & Ebringerova, 2000). The presence of a pyranose ring in the APS structure was depicted by a band at 612 cm⁻¹ (Yin, You, Jiang, & Zhou, 2016). Conclusively, this result shows that ultrasonic treatment had an insignificant effect on the chemical structure of the APS. In a previous study, Cui et al. (2018) observed unaltered chemical structures after ultrasound treatment.

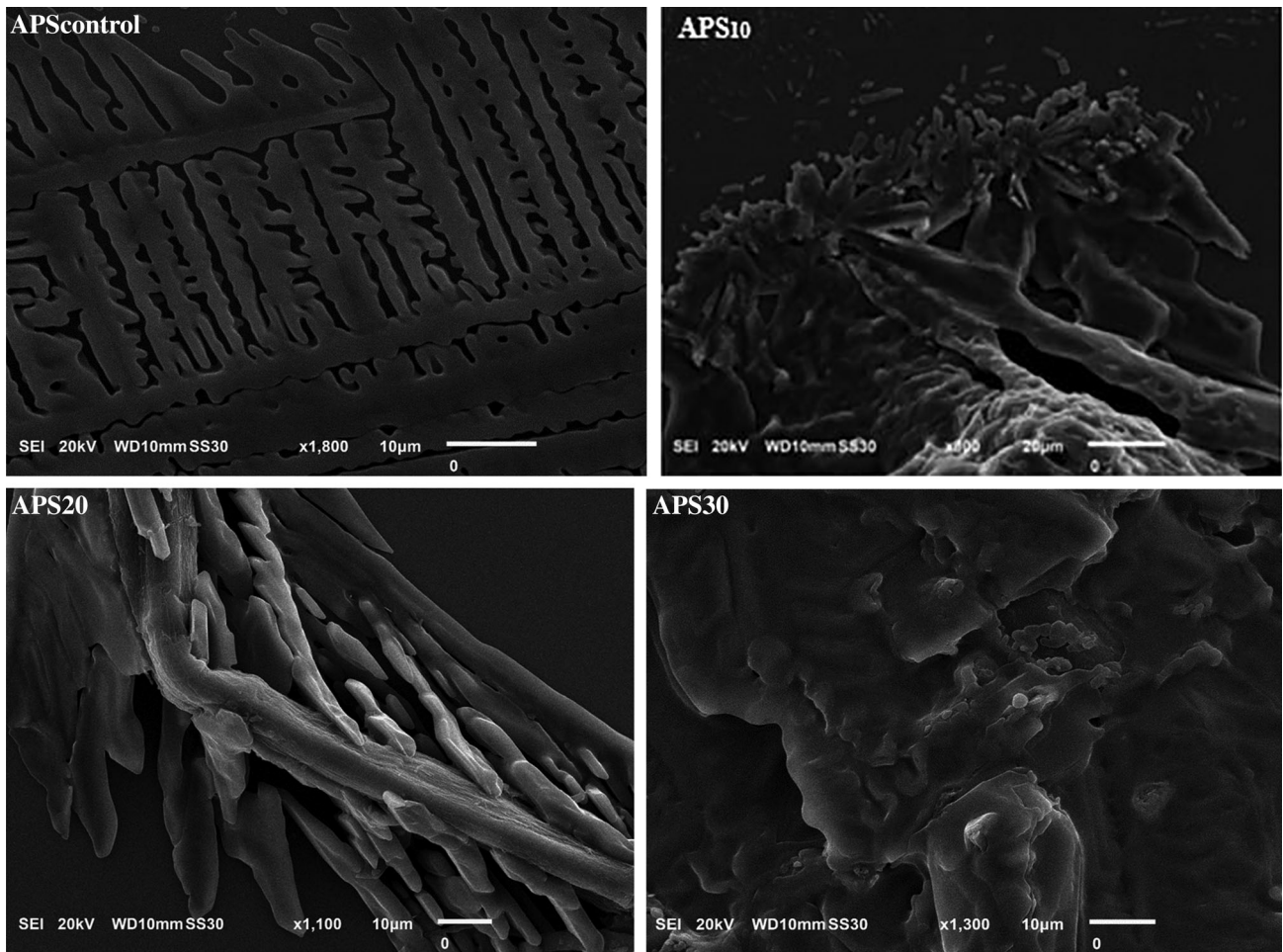


FIGURE 6 Scanning electron microscopy of non-sonicated APS_{control} and ultra-sonicated APS₁₀, APS₂₀, and APS₃₀

3.7.2 | UV-vis analysis

The outcome of this study revealed that the ATPS was effective in the removal of protein and nucleic acids from the salt-rich bottom

phase. As displayed in Figure 7b, no peaks were observed in the spectral range 260–280 nm. This signifies the non-existence of protein and nucleic acids and further confirms the deproteinization efficiency of the ethanol/(NH₄)₂SO₄ system as previously reported by

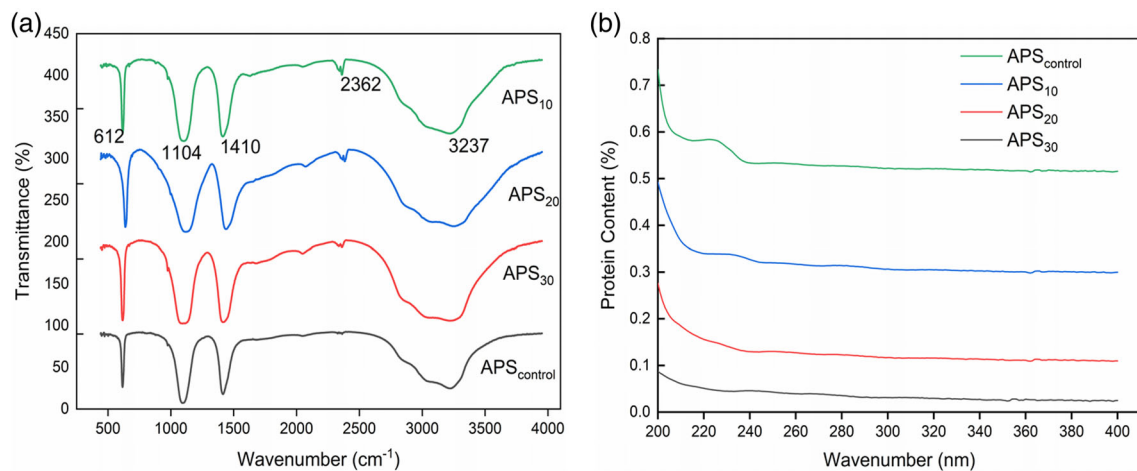


FIGURE 7 (a) Fourier transform Infrared Spectroscopy and (b) UV Vis spectral analysis of APS₁₀, APS₂₀, APS₃₀, and APS_{control}

(Wu et al., 2017). These results are line with the preliminary Bradford assay conducted as presented in Table 3.

3.8 | Anti-radical activities

3.8.1 | Hydroxyl scavenging

Hydroxyl radical ($\cdot\text{OH}$) is termed as one of the dominant reactive oxygen species causing oxidative degeneration and progression of cardiovascular diseases. Whilst reducing its dominance could greatly inhibit cellular impairments, it is worth exploring extraction mechanisms that retain the antioxidant potential of extracted compounds to stabilize radicals (Michiels, Kevers, Pincemail, Defraigne, & Dommes, 2012). Our results showed that there were significant ($p < .05$) differences between the APS samples at varied treatment times and concentrations. Through ultrasound extraction and desalination, the APS had positive substantial properties against the hydroxyl radical and this is shown by an increased inhibition (%) from 64.16% (control) to 68.75%, 70.39%, and 73.75% for the sonicated APS₁₀, APS₃₀, and APS₂₀, respectively as presented in Table 6. Polysaccharides eliminate the already existing hydroxyl radicals while also preventing the production of more radicals. In the current study dual-frequency, ultrasound might have created a strong cavitation effect which weakened

the cell wall and enabled the release of compounds consequently increasing the capacity of the APS to inhibit the production of $\cdot\text{OH}$ by donating compounds with $\cdot\text{OH}$ properties to stabilize the radicals (Shon, Kim, & Sung, 2003). Credibly, the physical and sonochemical effects of ultrasound treatment have been reported to improve the functionality of the sonicated extracts compared to other traditional extraction methods (Vilkhu, Mawson, Simons, & Bates, 2008). To reinforce this assertion, Chen et al. (2015) reported that APS extracted by the reflux method had a relatively weaker scavenging activity on the $\cdot\text{OH}$ radical compared to the APS extracts isolated using the combined enzyme method. Likewise, combined *Astragalus* and *Angelica* polysaccharides extracted using the hot water method were reported to have moderate effects on the hydroxyl radical (Pu et al., 2016). A comparison of the current study findings with the aforementioned showed that APS extracted under dual-frequency ultrasound had a greater potential to lower the proliferation of $\cdot\text{OH}$ radicals, and could greatly reduce oxidative impairments. This result is supported by Li et al. (2016) who have reported that ultrasonic disruption intensifies the degradation of high molecular weight polysaccharides to low molecular weight polysaccharides since low molecular weight polysaccharides possess a more reductive hydroxyl group to accept and eradicate free radicals (Leung, Zhao, Ho, & Wu, 2009). IC₅₀ value were reported as 0.42, 0.38, 0.43, and 0.56 mg/ml for APS₁₀, APS₂₀, APS₃₀, and APS_{control}, respectively.

Concentration (mg/ml)	APS ₁₀	APS ₂₀	APS ₃₀	APS _{control}
0.2	29.21 ± 0.63 ^b	32.86 ± 0.06 ^a	30.38 ± 1.33 ^b	25.22 ± 0.91 ^c
0.4	48.72 ± 0.90 ^{ab}	49.70 ± 1.25 ^a	46.35 ± 0.78 ^b	35.60 ± 0.71 ^c
0.6	53.65 ± 1.64 ^b	56.50 ± 0.47 ^a	53.06 ± 0.50 ^b	45.66 ± 0.45 ^c
0.8	58.68 ± 1.14 ^a	59.75 ± 2.37 ^a	57.16 ± 0.06 ^a	52.65 ± 1.27 ^b
1.0	60.97 ± 0.36 ^{ab}	62.37 ± 0.91 ^a	59.72 ± 1.49 ^b	56.03 ± 0.12 ^c
1.2	66.25 ± 0.22 ^a	67.75 ± 1.21 ^a	63.20 ± 1.23 ^b	62.69 ± 0.37 ^b
1.4	70.39 ± 0.83 ^b	73.75 ± 0.53 ^a	68.75 ± 0.34 ^b	64.16 ± 0.33 ^c

Notes: Means in the same row that do not share a letter are significantly different at $p < .05$. APS₁₀—ultrasound treatment (10 min), APS₂₀—ultrasound treatment (20 min), APS₃₀—ultrasound treatment (30 min), APS_{control}—ultrasound treatment (0 min).

TABLE 6 Hydroxyl scavenging activity of *Astragalus* polysaccharides

Concentration mg/ml	APS ₁₀	APS ₂₀	APS ₃₀	APS _{control}
0.2	19.79 ± 0.25 ^c	22.43 ± 0.20 ^a	21.60 ± 0.33 ^b	17.71 ± 0.23 ^d
0.4	27.54 ± 0.21 ^c	34.41 ± 0.20 ^a	30.37 ± 0.14 ^b	25.97 ± 0.53 ^d
0.6	39.32 ± 0.31 ^b	46.04 ± 3.07 ^a	41.78 ± 0.25 ^b	33.93 ± 0.26 ^c
0.8	50.59 ± 0.03 ^b	57.15 ± 1.66 ^a	55.73 ± 0.78 ^a	46.28 ± 0.55 ^c
1.0	57.22 ± 0.41 ^c	64.91 ± 0.23 ^a	61.91 ± 0.39 ^b	53.75 ± 0.55 ^d
1.2	68.59 ± 0.23 ^c	70.94 ± 0.11 ^a	69.53 ± 0.13 ^b	61.90 ± 0.47 ^d
1.4	74.78 ± 1.30 ^b	78.72 ± 0.16 ^a	72.13 ± 0.13 ^b	65.05 ± 0.11 ^c

Notes: Means in the same row that do not share a letter are significantly different at $p < .05$. APS₁₀—ultrasound treatment (10 min), APS₂₀—ultrasound treatment (20 min), APS₃₀—ultrasound treatment (30 min), APS_{control}—ultrasound treatment time (0 min).

TABLE 7 DPPH scavenging activity of *Astragalus* polysaccharides

3.8.2 | DPPH scavenging assay

The outcome of our study revealed that there was a significant difference ($p < .05$) amongst the APS samples at different concentrations and desalination treatment times. This is shown by the upsurge in the inhibition of DPPH (%) as shown in Table 7. The APS₂₀ sample exhibited higher DPPH scavenging power than the APS₁₀, APS₃₀, and APS_{control} samples, respectively. The results indicated that dual-frequency sonication had positive effects on the scavenging capacity of the APS against the DPPH radical. In an earlier study, APS that was synthesized with iron chloride hexahydrate was observed to have considerable scavenging properties on the DPPH radical (Lu et al., 2016). In another study, APS extracted using the reflux and hot water method did not have sizeable effects on lowering oxidation against the DPPH radical compared to the enzyme-treated extracts (Chen et al., 2014; Pu et al., 2016). The findings of these previous studies and the current study confirm the positive impact of sonication on the APS which might have undoubtedly increased the production and availability of proton donor compounds (Kedare & Singh, 2011). Furthermore, a synergistic effect of APS with other chemical compounds such as isoflavonoids, triterpene, and saponins which have been reported to have strong antioxidant properties could have explained the high scavenging capacity (Liu et al., 2015). The results in this study corroborate the findings of Yang, Jiang, Zhao, Shi, and Wang (2008) who reported that ultrasonic treatment increased the proton donation abilities of polysaccharides from *longan* fruit pericarp. Conversely, while ultrasonication is credited to increase the antioxidant activity of polysaccharides, prolonged exposure of the APS to the ultrasonic waves can influence degradation thus decreasing its bioactivity and scavenging potential. IC₅₀ values for all samples were reported as 0.64, 0.62, 0.66, and 0.72 mg/ml for APS₁₀, APS₂₀, APS₃₀, and APS_{control}, respectively.

3.9 | Mechanism of DFu-AATPE of *Astragalus* polysaccharides

To further understand the mechanism of dual-frequency ultrasound-assisted alcohol/salt aqueous two-phase extraction on the APS yield, a one-step approach with two distinct multiphase processes of mass transfers of the APS was designed. Initially, polysaccharide powders were added into the bottom phase of an ethanol/(NH₄)₂SO₄ ATPS. Subsequently, the powders settled on the interface of the two phases of the ATPS, allowing for the transfer of APS from the bottom to the top phase (Chen et al., 2016; Ji et al., 2018). In this process, the multiphase extraction of polysaccharides was characterized by the partitioning and transfer of less polar polysaccharides to the ethanol top phase while the polysaccharides with carboxylic groups transferred to the bottom phase. Next, the complex liquid-solid-liquid extraction occurred in the acoustic field which consequently led to an improved synergistic effect between the ultrasound waves and molecules. Ultrasonication using low and high frequencies immensely increases the surface area for reaction kinetics to occur, it also

increases the solvent/material interaction thus, increasing the transfer of molecules and improving extraction efficiencies (Chemat et al., 2017; Ji et al., 2018). Furthermore, ultrasonication significantly enhances the demixing effects of the ethanol/(NH₄)₂SO₄ which facilitates the partitioning of polysaccharides amongst the two phases based on their polarity (Chen et al., 2016). It is evident that the integration of dual-frequency ultrasound with the ATPS into a single-step process had multiple advantages over the traditional methods of extracting polysaccharides as it increased the APS yield and had a greater capacity to separate the water-soluble polysaccharides from the ethanol-soluble polysaccharides.

4 | CONCLUSION

Astragalus polysaccharides were simultaneously extracted and purified under a dual-frequency ultrasound-assisted ethanol/(NH₄)₂SO₄ aqueous two-phase system. The effects of dual frequency ultrasound-assisted desalination on the purified APS were also investigated. The outcome of this study revealed that dual-frequency ultrasound enhanced the polysaccharide yield to 28.40% which was correlated to the predicted yield of 29.19%. Ultrasound-assisted desalination improved the desalination rate, maintained the chemical structure of the purified APS and contributed to attaining low molecular weight polysaccharides which showed high scavenging power against the hydroxyl and the 2,2-diphenyl-1-picrylhydrazyl (DPPH) radicals. The thermodynamic analysis revealed that ultrasound extraction significantly contributed to attaining a non-spontaneous, irreversible and endothermic reaction process. Monosaccharide analysis revealed the existence of xylose, mannose, galactose, glucose, arabinose, rhamnose and ribose in the APS samples. Spectral analysis showed a uniform and similar spectrum in the APS₁₀, APS₂₀, and APS₃₀. However, the microstructural analysis revealed that continuous ultrasonic exposure beyond 10 min had adverse effects on the APS. The findings from this study demonstrated the efficiency of dual-frequency ultrasound in the extraction, purification, and desalination of *Astragalus* polysaccharide and show its feasibility for industrial application as it is a bio-friendly technique with shorter processing times and fewer energy costs.

ACKNOWLEDGMENT

This work was supported by the National Natural Science Foundation of China (Nos. 21676124 and 21878131).

CONFLICT OF INTEREST

The authors declare no potential conflict of interest.

ORCID

Fadzai Chikari  <https://orcid.org/0000-0003-3489-2652>

Phyllis Otu  <https://orcid.org/0000-0001-6042-7952>

REFERENCES

Agyemang, K., Han, L., Liu, E., Zhang, Y., Wang, T., & Gao, X. (2013). Recent advances in *Astragalus membranaceus* anti-diabetic research:

- Pharmacological effects of its phytochemical constituents. *Evidence-Based Complementary and Alternative Medicine*, 2013, 1–9.
- Bi, Y., & Wu, Z. (2010). Factors analysis of ultrasound combined with cellulose enzymatic extraction of total Astragalus polysaccharides. *Journal of Guangdong Pharmaceutical College*, 2, 134–137.
- Bradford, M. M. (1976). A rapid and sensitive method for the quantitation of microgram quantities of protein utilizing the principle of protein-dye binding. *Analytical Biochemistry*, 72(1–2), 248–254.
- Capelo-Martínez, J.-L. (2009). *Ultrasound in chemistry: Analytical applications*. Hoboken, NJ: John Wiley & Sons.
- Chemat, F., & Khan, M. K. (2011). Applications of ultrasound in food technology: Processing, preservation and extraction. *Ultrasonics Sonochemistry*, 18(4), 813–835.
- Chemat, F., Rombaut, N., Sicaire, A.-G., Meullemiestre, A., Fabiano-Tixier, A.-S., & Abert-Vian, M. (2017). Ultrasound assisted extraction of food and natural products. Mechanisms, techniques, combinations, protocols and applications. A review. *Ultrasonics Sonochemistry*, 34, 540–560.
- Chen, H., Zhou, X., & Zhang, J. (2014). Optimization of enzyme assisted extraction of polysaccharides from Astragalus membranaceus. *Carbohydrate Polymers*, 111, 567–575.
- Chen, R.-Z., Tan, L., Jin, C.-G., Lu, J., Tian, L., Chang, Q.-Q., & Wang, K. (2015). Extraction, isolation, characterization and antioxidant activity of polysaccharides from Astragalus membranaceus. *Industrial Crops and Products*, 77, 434–443.
- Chen, Z., Zhang, W., Tang, X., Fan, H., Xie, X., Wan, Q., ... Tang, J. Z. (2016). Extraction and characterization of polysaccharides from semen Cassiae by microwave-assisted aqueous two-phase extraction coupled with spectroscopy and HPLC. *Carbohydrate Polymers*, 144, 263–270.
- Cui, F.-J., Qian, L.-S., Sun, W.-J., Zhang, J.-S., Yang, Y., Li, N., ... Wu, D. (2018). Ultrasound-assisted extraction of polysaccharides from *Volvariella volvacea*: Process optimization and structural characterization. *Molecules*, 23(7), 1706.
- Dong, B., Yuan, X., Zhao, Q., Feng, Q., Liu, B., Guo, Y., & Zhao, B. (2015). Ultrasound-assisted aqueous two-phase extraction of phenylethanoid glycosides from *Cistanche deserticola* YC Ma stems. *Journal of Separation Science*, 38(7), 1194–1203.
- Dubois, M., Gilles, K. A., Hamilton, J. K., Rebers, P. t., & Smith, F. (1956). Colorimetric method for determination of sugars and related substances. *Analytical Chemistry*, 28(3), 350–356.
- Feng, D., Van Deventer, J., & Aldrich, C. (2006). Ultrasonic defouling of reverse osmosis membranes used to treat wastewater effluents. *Separation and Purification Technology*, 50(3), 318–323.
- Feng, R., Zhao, Y., Zhu, C., & Mason, T. (2002). Enhancement of ultrasonic cavitation yield by multi-frequency sonication. *Ultrasonics Sonochemistry*, 9(5), 231–236.
- Fu, J., Wang, Z., Huang, L., Zheng, S., Wang, D., Chen, S., ... Yang, S. (2014). Review of the botanical characteristics, phytochemistry, and pharmacology of Astragalus membranaceus (Huangqi). *Phytotherapy Research*, 28(9), 1275–1283.
- Goja, A. M., Yang, H., Cui, M., & Li, C. (2013). Aqueous two-phase extraction advances for bioseparation. *Journal of Bioprocessing and Biotechniques*, 4(1), 1–8.
- Guo, Y., Han, J., Zhang, D., Wang, L., & Zhou, L. (2012). An ammonium sulfate/ethanol aqueous two-phase system combined with ultrasonication for the separation and purification of lithospermic acid B from *Salvia miltiorrhiza* Bunge. *Ultrasonics Sonochemistry*, 19(4), 719–724.
- Guo, Y., Han, J., Zhang, D., Wang, L., & Zhou, L. (2013). Aqueous two-phase system coupled with ultrasound for the extraction of lignans from seeds of *Schisandra chinensis* (turcz.) Baill. *Ultrasonics Sonochemistry*, 20(1), 125–132.
- Guo, Y., & Wu, P. (2008). Investigation of the hydrogen-bond structure of cellulose diacetate by two-dimensional infrared correlation spectroscopy. *Carbohydrate Polymers*, 74(3), 509–513.
- Iqbal, M., Tao, Y., Xie, S., Zhu, Y., Chen, D., Wang, X., ... Shabbir, M. A. B. (2016). Aqueous two-phase system (ATPS): An overview and advances in its applications. *Biological Procedures Online*, 18(1), 18.
- Ji, X., Peng, Q., Yuan, Y., Liu, F., & Wang, M. (2018). Extraction and physicochemical properties of polysaccharides from *Ziziphus jujuba* cv. Muzao by ultrasound-assisted aqueous two-phase extraction. *International Journal of Biological Macromolecules*, 108, 541–549.
- Jin, M., Zhao, K., Huang, Q., & Shang, P. (2014). Structural features and biological activities of the polysaccharides from Astragalus membranaceus. *International Journal of Biological Macromolecules*, 64, 257–266.
- Kacurakova, M., Capek, P., Sasinkova, V., Wellner, N., & Ebringerova, A. (2000). FT-IR study of plant cell wall model compounds: Pectic polysaccharides and hemicelluloses. *Carbohydrate Polymers*, 43(2), 195–203.
- Kalinenko, O. S., Baklanov, A. N., & Makarov, V. A. (2016). *Using dual-frequency ultrasound in intensifying the stage of mineralization of plant and animal foods* (pp. 37–38). Germany: Deutscher Wissenschaftsverlag.
- Kedare, S. B., & Singh, R. (2011). Genesis and development of DPPH method of antioxidant assay. *Journal of Food Science and Technology*, 48(4), 412–422.
- Kwaw, E., Ma, Y., Tchabo, W., Apaliya, M. T., Xiao, L., & Wu, M. (2017). Effect of lactic acid fermentation on the phytochemical, volatile profile and sensory attributes of mulberry juice. *Journal of Food & Nutrition Research*, 56(4), 305–317.
- Leung, P. H., Zhao, S., Ho, K. P., & Wu, J. Y. (2009). Chemical properties and antioxidant activity of exopolysaccharides from mycelial culture of *Cordyceps sinensis* fungus Cs-HK1. *Food Chemistry*, 114(4), 1251–1256.
- Li, S., Xiong, Q., Lai, X., Li, X., Wan, M., Zhang, J., ... Guan, J. (2016). Molecular modification of polysaccharides and resulting bioactivities. *Comprehensive Reviews in Food Science and Food Safety*, 15(2), 237–250.
- Liau, M. Y., Natan, F., Widiyanti, P., Iksari, D., Indraswati, N., & Soetaredjo, F. (2008). Extraction of neem oil (*Azadirachta indica* A. Juss) using n-hexane and ethanol: Studies of oil quality, kinetic and thermodynamic. *ARPN Journal of Engineering and Applied Sciences*, 3(3), 49–54.
- Liu, D., Zhang, L., Xu, Y., & Zhang, X. (2013). The influence of ultrasound on the structure, rheological properties and degradation path of citrus pectin. Paper presented at the Proceedings of Meetings on Acoustics ICA2013.
- Liu, J., Wen, X.-Y., Zhang, X.-Q., Pu, H.-M., Kan, J., & Jin, C.-H. (2015). Extraction, characterization and in vitro antioxidant activity of polysaccharides from black soybean. *International Journal of Biological Macromolecules*, 72, 1182–1190.
- Liu, J., Zhu, J.-H., & Fan, J.-P. (2008). Application of detergent/polymer aqueous two phase systems for purification of membrane protein. *Jiangxi Science*, 3, 019.
- Lu, Q., Xu, L., Meng, Y., Liu, Y., Li, J., Zu, Y., & Zhu, M. (2016). Preparation and characterization of a novel Astragalus membranaceus polysaccharide-iron (III) complex. *International Journal of Biological Macromolecules*, 93, 208–216.
- Luo, A., He, X., Zhou, S., Fan, Y., Luo, A., & Chun, Z. (2010). Purification, composition analysis and antioxidant activity of the polysaccharides from *Dendrobium nobile* Lindl. *Carbohydrate Polymers*, 79(4), 1014–1019.
- Michiels, J. A., Kevers, C., Pincemail, J., Defraigne, J. O., & Dommes, J. (2012). Extraction conditions can greatly influence antioxidant capacity assays in plant food matrices. *Food Chemistry*, 130(4), 986–993.
- Muatasim, R., Ma, H., & Yang, X. (2018). Effect of multimode ultrasound assisted extraction on the yield of crude polysaccharides from *Lycium barbarum* (Goji). *Food Science and Technology*, 38, 160–166.
- Nimse, S. B., & Pal, D. (2015). Free radicals, natural antioxidants, and their reaction mechanisms. *RSC Advances*, 5(35), 27986–28006.

- Ogutu, F. O., Mu, T.-H., Elahi, R., Zhang, M., & Sun, H.-N. (2015). Ultrasonic modification of selected polysaccharides-review. *Journal of Food Processing & Technology*, 6(5), 1.
- Ooi, C. W., Tey, B. T., Hii, S. L., Kamal, S. M. M., Lan, J. C. W., Ariff, A., & Ling, T. C. (2009). Purification of lipase derived from *Burkholderia pseudomallei* with alcohol/salt-based aqueous two-phase systems. *Process Biochemistry*, 44(10), 1083–1087.
- Osae, R., Zhou, C., Tchabo, W., Xu, B., Bonah, E., Alenyorege, E. A., & Ma, H. (2019). Optimization of osmotic pretreatment of ginger (*Zingiber officinale* Roscoe) using response surface methodology: Effect on antioxidant activity, enzyme inactivation, phenolic compounds, and physical properties. *Journal of Food Process Engineering*, 42(10), 1–17.
- Otu, P. N. Y., Haonan, J., Cunshan, Z., & Hongpeng, Y. (2018). *Sorghum bicolor* L. leaf sheath polysaccharides: Dual frequency ultrasound-assisted extraction and desalination. *Industrial Crops and Products*, 126, 368–379.
- Peres, G. L., Leite, D. C., & Silveira, N. P. d. (2015). Ultrasound effect on molecular weight reduction of amylopectin. *Starch-Stärke*, 67(5–6), 407–414.
- Ponmurugan, K., Al-Dhabi, N. A., Maran, J. P., Karthikeyan, K., Moothy, I. G., Sivarajasekar, N., & Manoj, J. J. B. (2017). Ultrasound assisted pectic polysaccharide extraction and its characterization from waste heads of *Helianthus annuus*. *Carbohydrate Polymers*, 173, 707–713.
- Pu, X., Ma, X., Liu, L., Ren, J., Li, H., Li, X., ... Fan, W. (2016). Structural characterization and antioxidant activity in vitro of polysaccharides from angelica and astragalus. *Carbohydrate Polymers*, 137, 154–164.
- Salehi, F., Khashaninejad, M., Tadayyon, A., & Arabameri, F. (2015). Modeling of extraction process of crude polysaccharides from basil seeds (*Ocimum basilicum* L.) as affected by process variables. *Journal of Food Science and Technology*, 52(8), 5220–5227.
- Shon, M.-Y., Kim, T.-H., & Sung, N.-J. (2003). Antioxidants and free radical scavenging activity of *Phellinus baumii* (*Phellinus* of *Hymenochaetaceae*) extracts. *Food Chemistry*, 82(4), 593–597.
- Sun, H., Kang, B., Chai, Z., Sun, H., Du, H., Gao, J., ... Guo, L. (2017). Characterization of root-associated microbiota in medicinal plants *Astragalus membranaceus* and *Astragalus mongholicus*. *Annals of Microbiology*, 67(9), 587–599.
- Vilkhu, K., Mawson, R., Simons, L., & Bates, D. (2008). Applications and opportunities for ultrasound assisted extraction in the food industry—A review. *Innovative Food Science & Emerging Technologies*, 9(2), 161–169.
- Wang, D., Fan, B., Wang, Y., Zhang, L., & Wang, F. (2018). Optimum extraction, characterization, and antioxidant activities of polysaccharides from flowers of *Dendrobium devonianum*. *International Journal of Analytical Chemistry*, 2018, 1–8.
- Wang, J., Jia, J., Song, L., Gong, X., Xu, J., Yang, M., & Li, M. (2019). Extraction, structure, and pharmacological activities of *Astragalus* polysaccharides. *Applied Sciences*, 9(1), 122.
- Wang, J., Zhang, J., Zhao, B., Wang, X., Wu, Y., & Yao, J. (2010). A comparison study on microwave-assisted extraction of *Potentilla anserina* L. polysaccharides with conventional method: Molecule weight and antioxidant activities evaluation. *Carbohydrate Polymers*, 80(1), 84–93.
- Wang, X.-L., Li, X.-F., Fu, X.-Q., Chen, R., & Gao, B. (2005). Effect of ultrasound irradiation on polymeric microfiltration membranes. *Desalination*, 175(2), 187–196.
- Wang, Y., Han, J., Xu, X., Hu, S., & Yan, Y. (2010). Partition behavior and partition mechanism of antibiotics in ethanol/2-propanol-ammonium sulfate aqueous two-phase systems. *Separation and Purification Technology*, 75(3), 352–357.
- Wang, Y., Wang, C., & Guo, M. (2019). Effects of ultrasound treatment on extraction and rheological properties of polysaccharides from *Auricularia Cornea* var. *Li*. *Molecules*, 24(5), 939.
- Wang, Y., Zhang, X., Ma, X., Zhang, K., Li, S., Wang, X., ... Li, Y. (2019). Study on the kinetic model, thermodynamic and physicochemical properties of Glycyrrhiza polysaccharide by ultrasonic assisted extraction. *Ultrasonics Sonochemistry*, 51, 249–257.
- Wu, X., Li, R., Zhao, Y., & Liu, Y. (2017). Separation of polysaccharides from *Spirulina platensis* by HSCCC with ethanol-ammonium sulfate ATPS and their antioxidant activities. *Carbohydrate Polymers*, 173, 465–472.
- Yan, J.-K., Wang, Y.-Y., Qiu, W.-Y., Wang, Z.-B., & Ma, H. (2018). Ultrasound synergized with three-phase partitioning for extraction and separation of *Corbicula fluminea* polysaccharides and possible relevant mechanisms. *Ultrasonics Sonochemistry*, 40, 128–134.
- Yang, B., Jiang, Y., Zhao, M., Shi, J., & Wang, L. (2008). Effects of ultrasonic extraction on the physical and chemical properties of polysaccharides from longan fruit pericarp. *Polymer Degradation and Stability*, 93(1), 268–272.
- Yin, X., You, Q., Jiang, Z., & Zhou, X. (2016). Optimization for ultrasonic-microwave synergistic extraction of polysaccharides from *Cornus officinalis* and characterization of polysaccharides. *International Journal of Biological Macromolecules*, 83, 226–232.
- Ying, Z., Han, X., & Li, J. (2011). Ultrasound-assisted extraction of polysaccharides from mulberry leaves. *Food Chemistry*, 127(3), 1273–1279.
- Zhang, L., Ye, X., Ding, T., Sun, X., Xu, Y., & Liu, D. (2013). Ultrasound effects on the degradation kinetics, structure and rheological properties of apple pectin. *Ultrasonics Sonochemistry*, 20(1), 222–231.
- Zhang, Z.-S., Wang, L.-J., Li, D., Jiao, S.-S., Chen, X. D., & Mao, Z.-H. (2008). Ultrasound-assisted extraction of oil from flaxseed. *Separation and Purification Technology*, 62(1), 192–198.
- Zhao, C., Yang, C., Liu, B., Lin, L., Sarker, S. D., Nahar, L., ... Xiao, J. (2017). Bioactive compounds from marine macroalgae and their hypoglycemic benefits. *Trends in Food Science & Technology*, 72, 1.
- Zhao, Y.-M., Yang, J.-M., Liu, Y.-H., Zhao, M., & Wang, J. (2018). Ultrasound assisted extraction of polysaccharides from *Lentinus edodes* and its anti-hepatitis B activity in vitro. *International Journal of Biological Macromolecules*, 107, 2217–2223.
- Zhou, B., Zhang, M., Fang, Z.-X., & Liu, Y. (2015). Effects of ultrasound and microwave pretreatments on the ultrafiltration desalination of salted duck egg white protein. *Food and Bioprocesses Processing*, 96, 306–313.
- Zhu, Z.-Y., Liu, R.-Q., Si, C.-L., Zhou, F., Wang, Y.-X., Ding, L.-N., ... Zhang, Y.-M. (2011). Structural analysis and anti-tumor activity comparison of polysaccharides from *Astragalus*. *Carbohydrate Polymers*, 85(4), 895–902.
- Zhu, Z.-Y., Pang, W., Li, Y.-Y., Ge, X.-R., Chen, L.-J., Liu, X.-C., ... Zhang, Y. (2014). Effect of ultrasonic treatment on structure and antitumor activity of mycelial polysaccharides from *Cordyceps gunnii*. *Carbohydrate Polymers*, 114, 12–20.
- Zou, Y., Jiang, A., & Tian, M. (2015). Extraction optimization of antioxidant polysaccharides from *Auricularia auricula* fruiting bodies. *Food Science and Technology*, 35(3), 428–433.

How to cite this article: Chikari F, Han J, Wang Y, et al. Dual-frequency ultrasound-assisted alcohol/salt aqueous two-phase extraction and purification of *Astragalus* polysaccharides.

J Food Process Eng. 2020;43:e13366. <https://doi.org/10.1111/jfpe.13366>